Uhandisi Journal, Vol. 9, no.1, 1985

AN ELECTROHYDRODYNAMIC STUDY OF THE NEGATIVE CORONA ELECTRIC WIND

By

Henry Kadete*

ABSTRACT

The velocity of corona generated electric wind is measured. From the velocity profile mass movement and electrokinetic conversion efficiencies are deduced. High speed schlieren photographs illustrate the form of the velocity distribution function as well as its high degree of turbulence.

INTRODUCTION

The momentum transfer which occurs in the negative corona point-to-plate discharge configuration when negatively charged particle collide with neutral air molecules, results in the air motion generally referred to as "corona wind" or "electric wind", blowing away from the discharge point (1,2). The impingement of this wind on a surface, augments the rate of heat transfer across the surface (3). The heat transfer surface can be either the positive electrode itself or any object placed in the drift region of the discharge gap. The mechanism by which the heat transfer rate is influenced is still not well understood, inspite of there being a number of patents and practical applications in extistence (4). This paper is on a part of a study which should elucidate the mechanism of heat transfer augmentation by a negative corona electric wind with particular attention paid to its electrohydynamic characteristics.

2. BASIC PRINCIPLES

The MKS system of units and the conventional symbols are adopted. The fundamental equation for the corona electric wind, developed by Chattock (1) states that,

$$dF_x = \iiint \rho e E \, dy \, dz \, dx, \qquad (1)$$

Where dF_x is the force exerted on the ions of density ρ in a plane slab of width dx by an electric field E. The elementary charge e has the the value -1.602×10^{-19} C. The cartesian coordinate system is denoted by x in the direction of flow with y and z orthonormal to it. With the substitution $E = V_d/K$ where V_d is the ion drift velocity and K its mobility and another substitution $I_c = \iint V_d \rho e \, dy \, dz$, where I_c is the total corona current, Eq. (1) is reduced to the form

---

* Lecturer, Department of Electrical Engineering, University of Dar es Salaam.

$$dF_x = \frac{i_c}{K} dx$$

It is assumed that the current I_c is totally carried by negative irons. The above equation can be rewritten as

$$\frac{dp}{dx} = \frac{I_c}{KA} \qquad (2)$$

Where dp is the ion drag pressure difference developed across a differential distance dx by the corona current I_c flowing through an area A. From the ion drag pressure generated by the corona wind we obtain the wind velocity by applying Bernoulli's equation,

$$p + {}^1/_2 \rho_f v^2 + \rho_f gh = \text{constant} \qquad (3)$$

along a streamline, where p is the static pressure, ρ_f the mass density of the fluid, v the velocity along the streamline, g the acceleration of gravity and h the height of the point in question related to a zero level plane. In a situation where the height does not appreciably vary we find that

$$v = \sqrt{\frac{2\Delta p}{\rho_f}} \qquad (4)$$

In our case, v is the air velocity in the flow field, Δp is the pressure difference inside the flowfield to that outside it and ρ_f is the air density which has the value of 1.293 kg/m^3 at NTP. Here, Δp can be calculated from measurements with a Pitot tube according to the equation

$$\Delta p = \rho_i g \Delta h_p$$

Where ρ_i is the manometric fluid mass density in the Pitot tube, and Δh_p is the difference in the levels of the two fluid columns in the Pitot tube. A well known conversion of 1 pascal $\approx 10^{-4}$ m H_2O then applies.

Clearly Eq. (4) yields the spatial velocity distribution which may be obtained experimentally from measurement of the spatial dynamic pressure distribution.

This paper is addressed to a number of features of the corona wind.

a. Its velocity function will be studied in relationship to the corona current density at the plate which is often described by the empirical Warburg's current distribution (5),

$$j(\theta) = j(0) \cos^5 \theta \qquad (6)$$

Where j is the corona current density at any point r radially away from the discharge gap axis and θ equals $\tan^{-1}(r/H)$.

b. Since we are interested in the turbulence of the corona wind involved in convective heat transfer, an optical study with high speed photographic Toepler schlieren techniques is also made.

3. GENERAL THEORETICAL CONSIDERATIONS

A theoretical solution for the electrohydrodynamic flow field in an inhomogenous field discharge gap is presently too difficult due to two main reasons. Not only is the electric field very inhomogenous and divergent, being very high near the discharge point where its cross-section is small and falling to a very low value in the larger portion of the drift region where its cross-section is large, but more importantly the electric field is strongly modified due to the spatio-temporal dependence of the space charge density throughout the discharge period.

Generally two types of drift regions of negative corona discharges may be considered. The Trichel coronal current pulsed discharge with very little space charge at all, may be considered to have a field determined by the discharge gap geometry and the voltage applied across it. On the other had, an increase of the voltage will result into a space charge dominated field, referred to as the glow discharge, which is non pulsating. The Trichel pulses normally merge in time at a repetition rate of about 1 MHz.

The equations which describe the fields in the drift regions of these two types of discharges are

$$\text{grad}^2 U = D, \qquad E = -\text{grad}\, U, \tag{7}$$

for the former and

$$j = \rho e V_d \qquad = \rho e K E \qquad \text{curl}\, j = 0 \tag{8}$$

$$E = -\text{grad}\, U \qquad \text{grad}^2 U = -\rho e / \epsilon_0$$

$$\frac{D\rho}{Dt} = \frac{-K^2 \rho e}{\epsilon_0} \tag{9}$$

for the latter. Here ρ is the ion density and D/Dt stands for the so called hydrodynamic derivative as seen if one moves with the drifting ions.

Equation (9) is derived if we assume the relationship

$$\frac{\partial \rho}{\partial t} + \text{grad}.(V_d \rho) = \frac{\partial \rho}{\partial t} + V_d . \text{grad}\, \rho + \rho\, \text{grad}. V_d = 0$$

for the continuity equation.

4. EXPERIMENTS

a. Velocity Measurements

The electric wind system (EWS) consists of a flat stainless steel 90^0 edge as one discharge electrode and a flat wire mesh of 59.17% transparency as anode. Velocity measurements were made by a Pitot tube (6) having water as the manometric fluid and also fitted with an optical amplification mechanism. Two grounded parallel wires of 5 mm diameter were placed in between the discharge electrode and the plate for a number of experiments which

will be described later. The negative high dc voltage was supplied by a Wallis type dc high-voltage source, rated 0-30 kV dc, 0-1 mA. The high voltage circuit contained a 2 MΩ current limiting resistor for the protection of the source in case of a sparkover and a 4000 pF smoothing capacitor connected in parallel to the dc supply. A sensitive electrostatic voltmeters was used to measure the test gap voltage. Sensitive Keithley electrometers with current ranges from 100 fA - 3A were connected in series with the ground circuits of the anodes for the measurement of dc currents.

The actual wind velocity V in front of the wire mesh facing the discharge point was calculated from Eq. (4), where Δp_1 is the corrected value of the dynamic pressure. A correction was made for the pressure loss across the wire mesh itself in accordance to the following procedure: If Δp_2 is the dynamic pressure measured behind the mesh then $\Delta p_1 = (1 + X)$ Δp_2 is the dynamic pressure in front of the wire mesh as given by Jonas (7).

Here X, which is dimensionless, is the resistance coefficient of the wire mesh given by

$$X = 0.15 (1/\beta^4 - 1)\ 1/u_2 = 0.5 (1/\beta^2 - 1) \qquad (10)$$

where

$$u_2 = \frac{\sqrt{2\Delta p_2}}{\rho_f}$$

and β is the transparency of the wire mesh.

b. Schlieren Diagnostics

A conventional Toepler schlieren system (8) with high speed photography was employed. A 100 W quartz mercury vapour lamp with built in condenser lenses provided a beam of light which was focused at a pinhole of 0.5 mm diameter by a 40 mm diameter, 120 mm focal length lens. The pinhole then acted as the required light point source supplying a divergent beam of light 120 mm. The parallel beam of light was directed through the test gap to a schlieren head lens of 40 mm diameter and 120 mm focal length. A knife edge was positioned in the focal plane of the schlieren lens, to obstruct a part of the light source image.

High speed photographs were made with a Nikon camera shutter apparatus and a polaroid body or film carrier using black and white ASA 3000 polaroid films. The schlieren system is shown in Fig.1. The experiments were carried out on electric wind created in ambient air. The discharge electrode was screwed to the top of a soldering iron, which was subsequently heated by a 36 Vdc supply to produce the necessary temperature and density variations in the electric wind. Without this additional heating system the electric wind velocity was found to be too low to generate any discernible optical disturbances. If the knife edge cuts off a part of the light source image, the light intensity which illuminates the photographic plate will be reduced. Let a be the reduced height of the light sources image, and Δa a small increase of the height due to a optical disturbance in the test field caused by a density variation there. If the light source image width is assumed to be constant, it can be shown that the photographic plate will show a relative light intensity change.

$$\frac{\Delta I}{I} = \frac{\Delta a}{a} \qquad (11)$$

which can be shown to be equivalent to the relation

$$\frac{\Delta I}{I} = f_2/a \int_{x_1}^{x_2} \partial n/\partial y \, dx \qquad (12)$$

Where I is the light intensity at the photographic plate, f_2 is the focal length of the schlieren head lense, and n is the refractive index of the test field medium. The cartesian coordinate system is defined by x in the direction of the beam of light, and z along the knife edge. While the cross-section of the parallel beam of light through the test field defines our Schlieren image, Eq.(12) states that the light intensity contrast is a value proportinal to the integral of the gradient of the refractive index in the y direction, between x_1 and x_2, which are the boundaries of our test field.

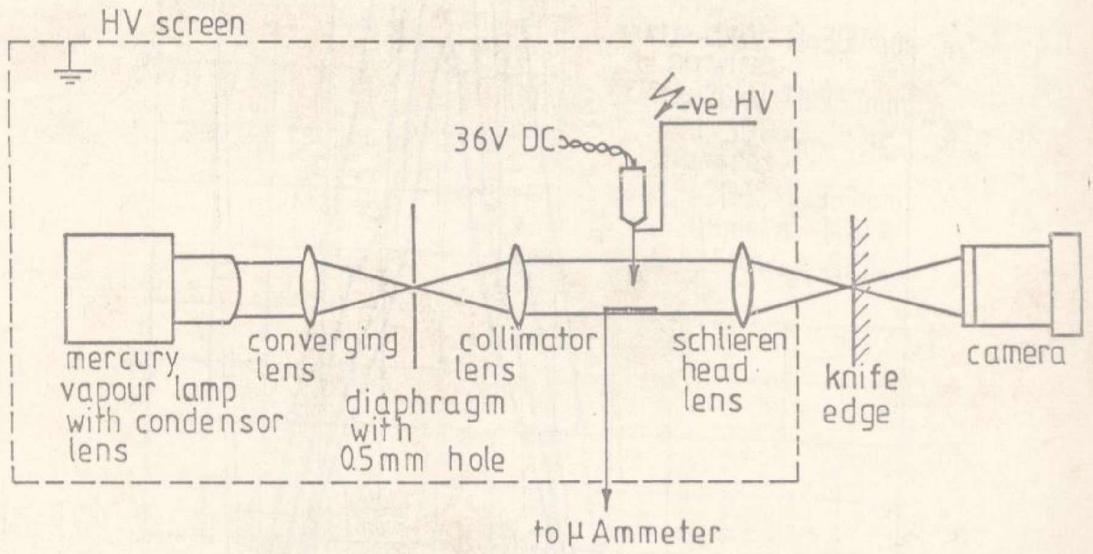

Fig.1. The Toepler schlieren system for the visualisation of the electric wind.

5. EXPERIMENTAL RESULTS

a. Velocity Measurements

Fig.2 shows a plot of the corona wind velocity v versus the radial displacement r. Fig.3 shows that the velocity distribution function has no similitude to the Warburg current distribution law. Measurements of the corona wind velocities with a Pitot tube indicates that the corona wind has a high degree of turbulence. The turbulence is less pronounced at larger radii; this is indicated by the vertical lines marked on the graph of Fig.3.

Placement of wires in between the point and the plate, parallel to the plate results in a velocity distribution function which is more spread out radially with increased velocity magnitudes as is shown in one of the graphs of Fig.2. The degree of change in the velocity profile depends on the position of the wires.

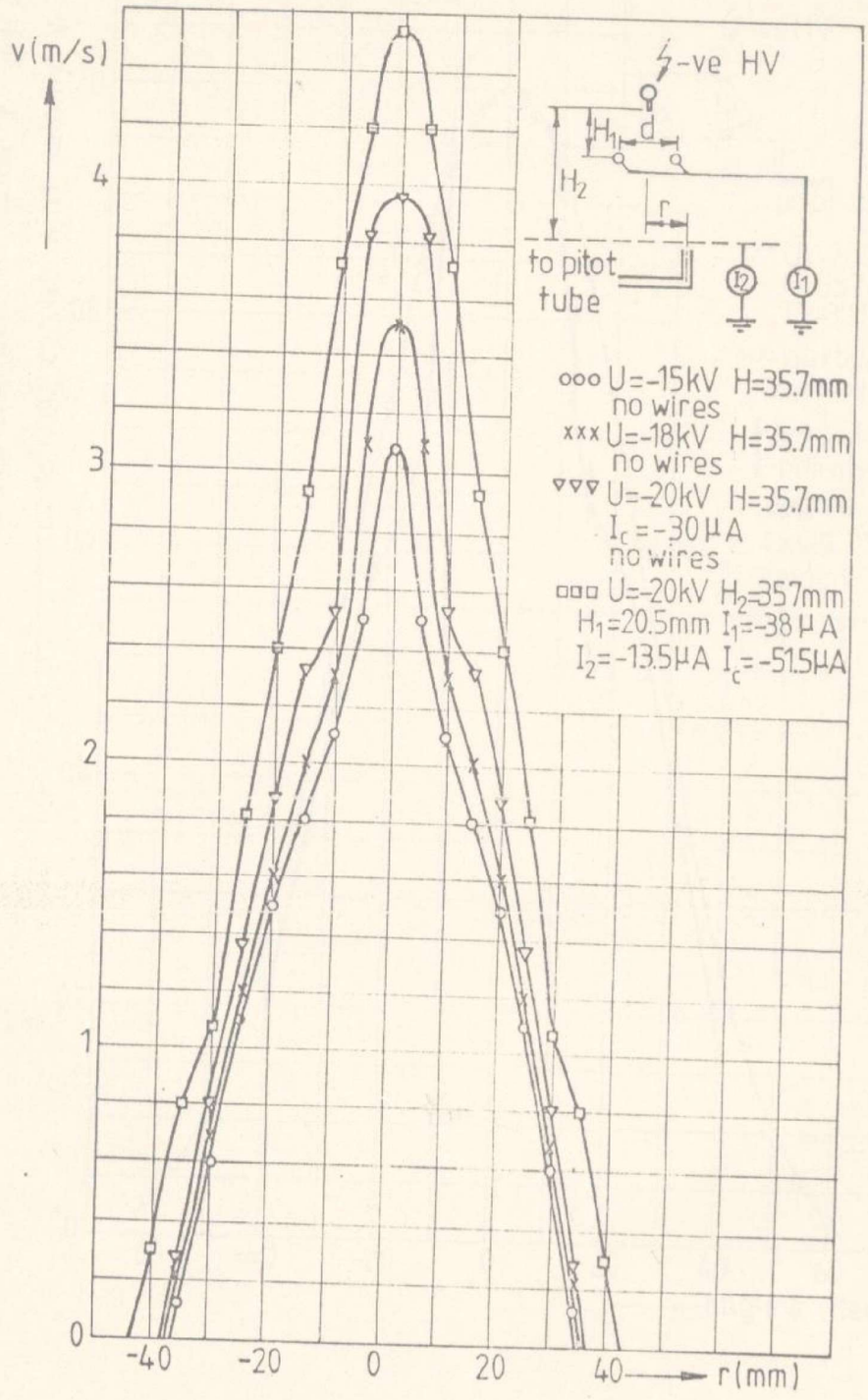

Fig.2. Corona wind velocity v vs radial distance r at the anode.

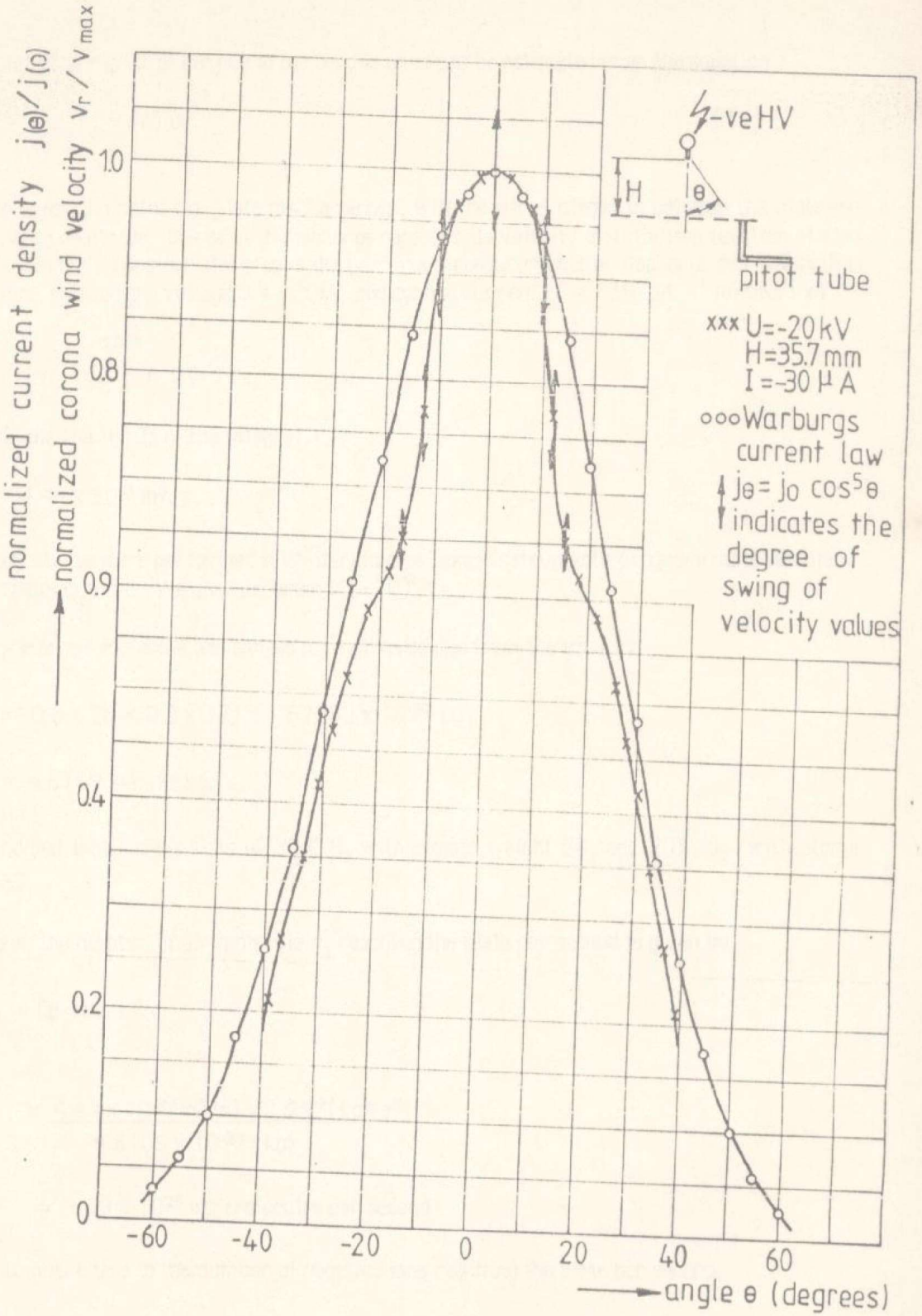

Fig.3. Normalized corona wind velocity $v(r)/v_{max}$ vs. angular displacement θ at the plate. A comparison is made with the Warburg's current density curve, $j(\theta) = j(0) \cos^5\theta$

The volume flow rate Q of air due to the corona wind can be estimated from the equation

$$Q = 2\pi \int r\, v(r)\, dr \qquad (13)$$

Let us consider the point-to-plate discharge gap, with no wires placed in between the plate and the discharge electrode. One of such discharge gaps has its velocity distribution function plotted in Fig.2. We shall consider the graphs derived from measurements of discharge gap of length H = 35.7 mm, applied gap voltage U = -20kV and corona current I_c = -30 μA. It follows that

$$Q = 2\pi \int_0^{0.038} r\, v(r)\, dr$$

See Fig.2 for the limits of the integral

$$Q \approx 4.44 \times 10^{-3}\ m^3/s$$

(All integrations were performed with the aid of a Texas Instruments programmable calculator TI Programmable 58. We used program ML-10).

On average an air molecule has a mass m_a approximated from the equation

$$m_a = (0.8 \times 28 + 0.2 \times 32) \times 1.67252 \times 10^{-27}\ kg$$

$$= 4.8169 \times 10^{-26}\ kg.$$

It is assumed that air consists of 80% N_2 with atomic weight 28, and 20% O_2 with atomic weight 32.

Therefore, the number of air molecule n_a reaching the plate per second is given by

$$n_a = Q\rho_f / m_a$$

$$= \frac{4.44 \times 10^{-3}(m^3/s) \times 1.293(kg/m^3)}{4.8169 \times 10^{-26}\ (kg)}$$

$$\approx 1.19 \times 10^{23}\ \text{air molecules per second.}$$

We can compare this to the number of negative ions reaching the plate per second,

$$n_e = I_c/e$$

$$= \frac{-30 \times 10^{-6}(a)}{-1.602 \times 10^{-19}(C)}$$

$$\approx 1.873 \times 10^{14}\ \text{ions per second.}$$

Therefore, for every ion there are about 6.35×10^8 neutral molecules which reach the plate.

An approximate value of the kinetic energy E_r possessed by the corona wind can be calculated from the equation

$$E_r = {}^1/_2 \rho_f \int 2\pi r v^3(r)\, dr \qquad (14)$$

in this case

$$E_r = {}^1/_2 \rho_f \int_0^{0.038} 2\pi r v^3(r)\, dr$$

See Fig. 2 for the limits of the integral.

Therefore

$$E_r = 7.6287 \times 10^{-3}\ J/s.$$

From this result of $E_r \approx 7.6287 \times 10^{-3}$ J/s, an electrokinetic conversion efficiency η, can be deduced as follows:

$$\eta = E_r/E_e \times 100\% \qquad (15)$$

Where $E_e = U \times I_c$, is the electrical power input to the gap

It follows that,

$$\eta = \frac{7.6287 \times 10^{-3}\ (J/s) \times 100\%}{-30 \times 10\text{-}6(A) \times -20 \times 103(V)}$$

$$\approx 1.27\%$$

The order of magnitude of electrokinetic conversion is in the range of 1%.

Now, let us consider a point-to-plate discharge gap with two parallel wires placed in between the discharge electrode and the plate. The velocity distribution function $v(r)$ of such a discharge gap is shown in one of the graphs of Fig.2. The discharge electrode was maintained at a distance $H_2 = 35.7$ mm from the plate. The wires, each of diameter $d_w = 5$mm, were place at a distance $H_1 = 20.5$ mm from the discharge electrode. The wires were at a distance of $d = 40$ mm. The voltage U applied between the discharge gap and ground was -20 kV. The two wires and the plate were grounded. A current $I_1 = 38\ \mu A$ was measured to flow into the plate. The volume flow rate Q of air in the corona wind of an electric wind system (EWS) described above can be calculated from Eq. 13. In this case,

$$Q = 2\pi \int_0^{0.043} r\, v(r)\, dr.$$

See Fig.2 for the limits of the integral.

Therefore,

$$Q \approx 8.38 \times 10^{-3}\ m^3/s.$$

Compared with the volume flow rate $Q = 4.44 \times 10^{-3} m^3/s$ when the EWS had no wires, we see an increase in the volume flow rate of approximately 88%. This compares favourably to an increase of 70% in the total corona current i_c from 30 μA to 51.3 μA.

The kinetic energy of the corona wind E_r of the EWS with parallel wires can also be calculated from Eq. 14. In this case

$$E_r = {}^1/_2 \rho_f 2\pi \int_0^{0.043} r\, v^3(r)\, dr$$

See Fig. 2 for the limits of the integral.

Therefore,

$$E_r \approx 3.51 \times 10^{-2}\ J/s.$$

It follows therefore that the electrokinetic conversion efficiency for the EWS which contains wires is given by Eq. (15). In this case.

$$\eta = E_r/E_e \times 100\%.$$

$$= \frac{3.51 \times 10^{-2}(J/s) \times 100\%}{-51.3 \times 10^{-6}\,(A) \times -20 \times 10^{3}\,(v)}$$

$$\eta \approx 3.42\%$$

b. Schlieren diagnostics

The pictures taken of a corona wind showed that the narrow jet moves from the HV electrode (footpoint) where it is firmly anchored and proceeds to the plate (head) where it was observed to move about radially. This is at least one of the contributions for the highly-fluctating values observed when the wind velocity was measured with a Pitot tube.

6. CONCLUSIONS

a. From the graphs of Fig.3, we conclude that no similitude exists between this function and the Warburg's current distribution law. We therefore disagree with Thanh's (9) assertion.

b. The electric wind consists primarily of neutrals. For every negative particle which reaches the plate there arrive neutrals in the order of 10^8.

c. The electrokinetic conversion efficiency of a corona discharge in air is very low, namely of the order of 1%. The rest of the electricial power is expended in the form of light, sound, excitation of neutral, attachment of electrons to neutrals, ionization and heat.

d. Placement of parallel wires between a point and a plate increases the volume flow rate of air and improves the electrokinetic conversion efficiency. From our experimental data we calculated a rise in the volume flow rate of 88%. We also calculated a rise in the electrokinetic conversion efficiency from 1./27% to 3.42%.

e. Pitot tube velocity measurements have indicated that the corona wind is very turbulent. Schlieren diagnostics have shown that the radial movements of the corona wind jet contribute to the turbulence noticed when we measured the corona wind velocity with a Pitot tube.

7. REFERENCES

1. Chattock, A.P., "On the velocity and mass of the ions in the electric wind in air", Phil. Mag., vol.48 no.244, pp.401 - 420, 1899.

2. Loeb, L.B., Fundamentals of Electricity and Magnetism. Chapman and Hall, London, 1955, pp. 192 - 194.

3. O'Bried, R.J., and A.J. Shine, "Some effects of an electric field on heat transfer from a vertical plate in free convection", Trans. of the ASME, J. Heat Trans., pp.114-116, Febr. 1967.

4. Velkoff, H.R., and F.A. Kulacki, "Electrostatic cooling", ASME publication, Design Engineering Conference and Show, Chicago, pp. 1-6, May 1977.

5. Goldman, M., and R.S. Sigmond, "Corona and Insulation", IEEE Trans. EI, vol. EI-17, no.2, pp. 90-105, April, 1982.

6. Duckworth, R.A., Mechanics of Fluids. Longmans, London, 1977, pp.86-87.

7. Jonas, R., "The changes produced in an air stream by wire gauze", The Engineers Digest, vol.18, no.5, pp. 191-193, May 1957.

8. Merzkirch, W., Flow Visualization. Academic Press, New York, 1974, pp. 86-100.

9. Thanh, L.C. "Similitude between ionic wind, discharge pattern and corona current", Electr. letters, vol.5, no.2. pp.57-58, 1978.